Int. J. Heat Mass Transfer. Vol. 15, pp. 235–246. Pergamon Press 1972. Printed in Great Britain

LAMINAR FILMWISE CONDENSATION OF FLOWING VAPOUR ON A HORIZONTAL CYLINDER

TETSU FUJII, HARUO UEHARA and CHIKATOSHI KURATA*

Research Institute of Industrial Science, Kyūshū University, Fukuoka, Japan

(*Received* 22 *June* 1970)

Abstract—Two-phase boundary layer equations of filmwise condensation on a horizontal cylinder are solved with an approximate method due to Jacobs. Numerical results for average coefficients of heat transfer are expressed as; for downward vapour flow,

$$Nu = \chi\left(1 + \frac{0{\cdot}276}{\chi^4 FrH}\right)^{\frac{1}{4}} Re^{\frac{1}{4}},$$

especially for large vapour velocity, namely for $\frac{gD}{U_\infty^2 H} \ll \frac{\chi^4}{0{\cdot}276}$, $Nu = \chi Re^{\frac{1}{4}}$,

where

$$\chi = 0{\cdot}9\left(1 + \frac{1}{RH}\right)^{\frac{1}{4}}.$$

The heat transfer coefficients predicted by these expressions are in good agreement with experimental data, which are taken by the authors and Berman–Tumanov. Temperature distribution on the cylinder is usually affected by oncoming vapour velocity and surface heat flux, then the peripheral mean temperature must be adopted as the representative one.

NOMENCLATURE

A_0, A_2, B_1, coefficients in (45), (46);
c_p, specific heat at constant pressure;
D, outer diameter of a cylinder;
f, Froude number defined by (13);
Fr, Froude number defined by (44);
g, gravitational acceleration;
Gr, Grashof number defined by (52);
H, nondimensional number of condensation defined by (14);
L, latent heat of condensation;
Nu, average Nusselt number defined by (41);
Nu_{exp}, average Nusselt number experimented;
Pr, Prandtl number;
q, heat flux;
r, radius of a cylinder;
R, $\rho\mu$-ratio defined by (38);
Re, Reynolds number defined by (43);
T_i, measured temperature of the tube wall;
T_m, mean value of T_i;
T_s, temperature of saturated vapour;
T_w, surface temperature of a cylinder;
U, V, nondimensional velocities of vapour defined by (10) and (12) respectively;
U_∞, oncoming velocity of steam;
u, v, nondimensional velocities of condensate defined by (9) and (11) respectively;
y, z, nondimensional coordinate variables defined by (7) and (6) respectively.

* Now at Thechnical Research Laboratory, Kawasaki Heavy Industry Co., Kōbe, Japan.

Greek symbols

α, coefficient of heat transfer defined by (39) or (40);
Δ, nondimensional thickness of the vapour boundary layer defined by (28);
δ, nondimensional thickness of the liquid layer defined by (8);
ζ, nondimensional coordinate variable defined by (27);
λ, thermal conductivity;
μ, dynamic viscosity;
ν, kinematic viscosity;
ρ, density;
φ, angle measured clockwisely from the leading stagnation point;
χ, nondimensional number defined by (54).

Subscripts

1, dimensional value as shown in Fig. 1;
D, peripheral mean value;
φ, local value at angle φ;
Δ, value outside the vapour boundary layer;
δ, value at the interface between vapour and liquid.

Physical properties with and without superscripts $^-$ are for vapour and liquid respectively.

1. INTRODUCTION

LAMINAR filmwise condensation on a horizontal cylinder placed in quiescent vapour was solved by Nusselt [1] approximately. A more accurate solution of the boundary layer equation of the condensate film was obtained by Sparrow–Gregg [2] on account of both inertia and convection term. Furthermore, Chen [3] solved the two-phase boundary layer equation concerning the same problem. Similarly to the case of a vertical surface, however, these two solutions are almost coincident with Nusselt's approximate one, as far as the vapour is at atmospheric pressure or at room temperature except for metal vapours. Comparing the Nusselt's prediction with experimental data, McAdams [4] showed that measured values of heat transfer coefficients ran from 36 per cent below to 70 per cent above those predicted from the measured values of temperature differences and that the average of the ratio of measured to predicted coefficients was 1·23 for steam and 0·94 for organic vapours. Recent experimental data of Štěpánek *et al.* [5] exhibit that Nusselt's prediction is verified within the error of 10 per cent at least for benzen and methanol.

For condensation on vertical banks of horizontal tubes, Nusselt calculated the decreasing ratios of heat transfer coefficients toward lower tubes, assuming that the liquid film falls continuously from the upper tube to the lower one. Chen [3] gave a supplementary expression for these results on account of the effect of condensation between tubes. The experimental results for Freon-11 by Short–Brown [6] and for Freon-12 by Young–Wohlenberg [7], however, exhibited that these theoretical results predicted too low values. Though Chen noted that the phenomenon had been attributed to splashing and nonuniform spilling of the condensate, the effect of vapour velocity must be accounted first of all. Because each condenser tube has a function of a sink of vapour, the vapour velocity at the inlet of the tube bank becomes larger as the number of the tubes increases.

In this paper the effect of vapour velocity on condensation is studied with a single horizontal tube. Already, Sugawara *et al.* [8] and Shekriladze–Gomelauri [9] dealt with this problem, assuming that the shearing stress on the film surface was analogous to the case of noncondensing flow and to the case of the boundary layer with suction respectively. Recently Denny–Mills [10] gave somewhat accurate results under the same assumption as Shekriladze–Gomelauri's. The authors attempted to solve the two-phase boundary layer equations, assuming that vapour outside its boundary layer is potential flow. The reliability of both the method of solution and accompanying various assumptions was confirmed in previous paper [11]. A

simple expression for average coefficients of heat transfer is proposed and compared with experimental results.

2. BASIC EQUATIONS

Figure 1 shows the physical model and coordinate system. Vapour flow outside the boundary layer is assumed to be a potential one which is expressed by $2U_\infty \sin\varphi$. Other conditions and assumptions are similar to the case of a vertical surface already reported by the authors [11].

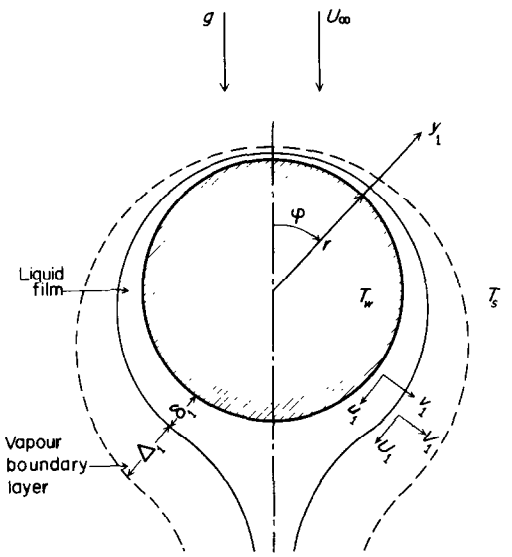

FIG. 1. Physical model and coordinate system.

Partinent equations are for the liquid film,

$$\frac{\partial u_1}{r\partial\varphi} + \frac{\partial v_1}{\partial y_1} = 0, \quad \text{(continuity)} \tag{1}$$

$$\nu\frac{\partial^2 u_1}{\partial y_1^2} + g\sin\varphi = 0, \quad \text{(momentum)} \tag{2}$$

$$\delta_1\frac{\mathrm{d}}{r\,\mathrm{d}\varphi}\int_0^{\delta_1} u_1\,\mathrm{d}y_1 = \frac{\lambda(T_s - T_w)}{\rho L}, \quad \text{(heat balance)} \tag{3}$$

for the vapour boundary layer,

$$\frac{\partial U_1}{r\partial\varphi} + \frac{\partial V_1}{\partial y_1} = 0, \quad \text{(continuity)} \tag{4}$$

$$U_1\frac{\partial U_1}{r\partial\varphi} + V_1\frac{\partial V_1}{\partial y_1} = \bar{\nu}\frac{\partial^2 U_1}{\partial y_1^2} + \frac{2U_\infty^2}{r}\sin 2\varphi. \quad \text{(momentum)} \tag{5}$$

For convenience of solving, pressure term in (2) $(2\bar{\rho}U_\infty^2/r)\sin 2\varphi$ is neglected. The validity will be discussed later.

By using following variables and numbers of nondimension,

$$z = \frac{\varphi}{f}, \quad y = y_1\left(\frac{g}{\nu U^2}\right)^{\frac{1}{3}}, \quad \delta = \delta_1\left(\frac{g}{\nu U_\infty^2}\right)^{\frac{1}{3}}, \tag{6), (7), (8)}$$

$$u = \frac{u_1}{U_\infty}, \quad U = \frac{U_1}{U_\infty}, \tag{9), (10)}$$

$$v = v_1\left(\frac{U_\infty}{\nu g}\right)^{\frac{1}{3}}, \quad V = V_1\left(\frac{U_\infty}{\nu g}\right)^{\frac{1}{3}}. \tag{11), (12)}$$

$$f = \frac{U_\infty^2}{gr}, \quad H = \frac{c_p(T_s - T_w)}{PrL}, \tag{13), (14)}$$

(1)–(5) are transformed as

$$\frac{\partial u}{\partial z} + \frac{\partial v}{\partial y} = 0, \tag{15}$$

$$\frac{\partial^2 u}{\partial y^2} + \sin fz = 0, \tag{16}$$

$$\delta\frac{\mathrm{d}}{\mathrm{d}z}\int_0^{\delta} u\,\mathrm{d}y = H, \tag{17}$$

$$\frac{\partial U}{\partial z} + \frac{\partial V}{\partial y} = 0, \tag{18}$$

$$U\frac{\partial U}{\partial z} + V\frac{\partial U}{\partial y} = \frac{\bar{\nu}}{\nu}\frac{\partial^2 U}{\partial y^2} + 2f\sin 2fz. \tag{19}$$

Boundary conditions and compatability ones at vapour–liquid interface for these equations are,

$$y = 0; \quad u = v = 0, \quad T = T_w, \tag{20}$$

$$y = \delta; \quad u = U = u_\delta = U_\delta, \tag{21}$$

$$\mu\left(\frac{\partial u}{\partial y}\right)_\delta = \bar{\mu}\left(\frac{\partial U}{\partial y}\right)_\delta, \tag{22}$$

$$\rho\left(u\frac{\mathrm{d}\delta}{\mathrm{d}z} - v\right)_\delta = \bar{\rho}\left(U\frac{\mathrm{d}\delta}{\mathrm{d}z} - V\right)_\delta, \tag{23}$$

$$T = T_s, \tag{24}$$

$$\zeta = \Delta; \quad U = U_\Delta = 2\sin fz, \qquad \left(\frac{\partial U}{\partial y}\right)_\Delta = 0, \tag{25), (26}$$

where

$$\zeta = y - \delta, \quad \Delta = \Delta_1\left(\frac{g}{\nu U_\infty}\right)^{\frac{1}{3}}, \tag{27), (28}$$

and the left-hand term of (23) is rewritten by using (15) and (17) as

$$\rho\left(u\frac{\mathrm{d}\delta}{\mathrm{d}x} - v\right)_\delta = \rho\frac{\mathrm{d}}{\mathrm{d}z}\int_0^\delta u\mathrm{d}y = \frac{\rho H}{\delta}. \tag{29}$$

Integrating (16) subject to (20) and (21) twice with respect to y, we obtain the velocity profile in the liquid film

$$u = \left(\frac{u_\delta}{\delta} + \frac{\delta}{2}\sin fz\right)y - \frac{\sin fz}{2}y^2. \tag{30}$$

When the velocity profile in the vapour boundary layer is approximated by a quadratic formula of ζ subject to (21), (25) and (26), it is expressed as

$$U = u_\delta + (2\sin fz - u_\delta)\left(\frac{2\zeta}{\Delta} - \frac{\zeta^2}{\Delta^2}\right). \tag{31}$$

Integrating (18) and (19) subject to (21), (25) and (26) with respect to y, we obtain respectively,

$$\frac{\mathrm{d}}{\mathrm{d}z}\int_\delta^{\delta+\Delta} U\,\mathrm{d}y - U_\Delta\frac{\mathrm{d}(\delta+\Delta)}{\mathrm{d}z} + u_\delta\frac{\mathrm{d}\delta}{\mathrm{d}z} + (V_\Delta - V_\delta) = 0, \tag{32}$$

$$\frac{\mathrm{d}}{\mathrm{d}z}\int_\delta^{\delta+\Delta} U^2\,\mathrm{d}y - U_\Delta^2\frac{\mathrm{d}(\delta+\Delta)}{\mathrm{d}z} + u_\delta^2\frac{\mathrm{d}\delta}{\mathrm{d}z} + (U_\Delta V_\Delta - u_\delta V_\delta) = -\frac{\bar{\nu}}{\nu}\left(\frac{\partial U}{\partial y}\right)_\delta + 2f\Delta\sin 2fz. \tag{33}$$

Taking operation (33)–U_Δ (32), and then transforming with (27), (23) and (29), we obtain

$$\frac{\mathrm{d}}{\mathrm{d}z}\int_0^\Delta U^2\mathrm{d}\zeta - U_\Delta\frac{\mathrm{d}}{\mathrm{d}z}\int_0^\Delta U\mathrm{d}\zeta - (U_\delta - U_\Delta)\frac{\rho H}{\bar{\rho}\delta} + \frac{\bar{\nu}}{\nu}\left(\frac{\partial U}{\partial \zeta}\right)_0 - 2f\Delta\sin 2fz = 0. \tag{34}$$

The ratio of Δ to δ is obtained by substituting (30) and (31) into (22), such that

$$\frac{\Delta}{\delta} = \frac{4\bar{\mu}(2\sin fz - u_\delta)}{\mu(2u_\delta - \delta^2\sin fz)}. \tag{35}$$

Substituting (30) into (17) and (31) and (35) into (34), we obtain respectively as

$$H = \left(\frac{u_\delta}{4} + \frac{\delta^2}{8}\sin fz\right)\frac{\mathrm{d}\delta^2}{\mathrm{d}z} + \frac{\delta^2}{2}\frac{\mathrm{d}u_\delta}{\mathrm{d}z} + \frac{\delta^4}{12}f\cos fz, \tag{36}$$

$$\begin{aligned}
&\tfrac{1}{2}(3u_\delta^2 - 2\sin fz - 8\sin^2 fz)(2\sin fz - u_\delta)\\
&\quad\times(2u_\delta + \delta^2\sin fz)\frac{\mathrm{d}\delta^2}{\mathrm{d}z} + [2\delta^2(3u_\delta - \sin fz)\\
&\quad\times(2\sin fz - u_\delta)(2u_\delta - \delta^2\sin fz)\\
&\quad-\delta^2(3u_\delta^2 - 2u_\delta\sin fz - 8\sin^2 fz)\\
&\quad\times(4 - \delta^2)\sin fz]\frac{\mathrm{d}u_\delta}{\mathrm{d}z} + fu_\delta\delta^2(4 - \delta^2)\\
&\quad\times(3u_\delta^2 - 2u_\delta\sin fz - 8\sin^2 fz)\cos fz\\
&\quad+4f\delta^2(2u_\delta - 9\sin fz)(2\sin fz - u_\delta)\\
&\quad\times(2u_\delta - \delta^2\sin fz)\cos fz + \tfrac{15}{8}R^2\\
&\quad\times[2(H+1)u_\delta - (4H + \delta^2)\sin fz]\\
&\qquad\times(2u_\delta - \delta^2\sin fz)^2 = 0.
\end{aligned} \tag{37}$$

where

$$R = (\rho\mu/\bar{\rho}\bar{\mu})^{\frac{1}{3}}. \tag{38}$$

When u_δ, δ are solved simultaneously from (36) and (37), local and average coefficient of heat transfer α_φ, α_D and average Nusselt number Nu are calculated by the following formula respectively,

$$\alpha_\varphi = \frac{q_\varphi}{(T_s - T_w)} = \frac{\lambda}{\delta_1} = \frac{\lambda}{\delta}\left(\frac{g}{\nu U_\infty}\right)^{\frac{1}{2}}, \quad (39)$$

$$\alpha_D = \frac{q_D}{(T_s - T_w)} = \frac{\lambda}{\delta_D}\left(\frac{g}{\nu U_\infty}\right)^{\frac{1}{2}}, \quad (40)$$

$$Nu = \frac{\alpha_D D}{\lambda} = \frac{1}{\delta_D}\left(\frac{Re}{Fr}\right)^{\frac{1}{2}}, \quad (41)$$

where

$$\frac{1}{\delta_D} - \frac{1}{\pi}\int_0^\pi \frac{1}{\delta}\,\mathrm{d}\varphi, \quad Re = \frac{U_\infty D}{\nu}, \quad (42), (43)$$

$$Fr = \frac{U_\infty^2}{gD}. \quad (44)$$

Integration of (36) and (37) cannot but be performed numerically for prescribed values of $f(= 2Fr)$, H and R. Because $z = 0$ is a singular point, u_δ and δ^2 are expanded in power series of z subject to physical conditions $u_\delta = 0$ and $\mathrm{d}\delta^2/\mathrm{d}z = 0$ at $z = 0$, such that

$$\delta^2 = A_0 + A_2 z^2 + \ldots, \quad (45)$$

$$u_\delta = B_1 z + B_3 z^3 + \ldots, \quad (46)$$

and $\sin fz$, $\cos fz$ are also approximated as

$$\sin fz \approx fz, \quad \cos fz \approx 1 - \tfrac{1}{2} f^2 z^2. \quad (47)$$

Substituting (45)–(47) into (36), we obtain

$$B_1 = \frac{2H}{A_0} - \frac{f}{6}A_0, \quad A_2 = \frac{f^3 A_0^3}{24B_1 + 10fA_0}, \quad (48)$$

then, substituting into (37) and eliminating B_1 with (48),

$$\begin{aligned} &f^3A_0^6 + 6f^3A_0^5 + \{-36f^2(8f + H) \\ &\quad + 30R^2f^2(H + 4)\}A_0^4 + \{-144f^2(18f + H) \\ &\quad + 360R^2Hf^2]A_0^3 + \{432fH(8f + H) \\ &\quad - 90R^2fH(5H + 8)\}A_0^2 \\ &\quad + \{864fH^2 - 1080R^2fH^2\}A_0 \\ &\quad + \{-1728H^2 + 1080R^2H^2(H + 1)\} = 0. \end{aligned} \quad (49)$$

Among two real and positive roots of (49) there is adopted the smaller one, because A_0, which is corresponding to the square of film thickness at $z = 0$, must be smaller than a double root for the case of $U_\infty = 0$. In the range of $z < 10^{-6} \sim 10^{-5}$, the first terms in (45) and (46) are employed, and in the larger range (36) and (37) are successively computed by means of Runge–Kutta–Gill method.

3. NUMERICAL RESULTS AND CONSIDERATIONS

Combinations of parameters R, H and Fr employed for numerical calculation are shown in Table 1 with the results for average coefficients of heat transfer. Peripheral distributions of the nondimensional coefficients of heat transfer are shown in Fig. 2. For the case that the vapour velocity or Fr is smaller, the temperature difference or H is larger, and the vapour pressure or $1/R$ is lower, both the local coefficients near the leading stagnation and the average coefficients become smaller.

Table 1. Parameters employed for numerical calculation and the results for average Nusselt number

No.	Symbol	R	$H \times 10^4$	$Fr \times 10^{-4}$	$Nu/\sqrt{Re}$
1	◇	10	1	0·5	8·960
2	○	1000	1	50	1·901
3	⊤	1000	1	5	1·977
4	○	1568	6·325	7·289	1·065
5	⊕	1568	6·325	3·571	1·068
6	⊕	1568	6·325	0·656	1·106
7	◐	1568	6·325	0·018	1·387
8	△	10000	1	0·500	1·127
9	▲	10000	10	0·005	1·601

In Fig. 3 the peripheral distributions of the local coefficients of heat transfer normalized by each average one are compared among three typical cases of high vapour velocity (No. 4), moderate one (No. 7) and quiescent vapour (Nusselt's prediction). For the case of high vapour velocity, about 78 and 98 per cent of total condensate take place where angle φ are less than 90 and 140 degrees respectively.

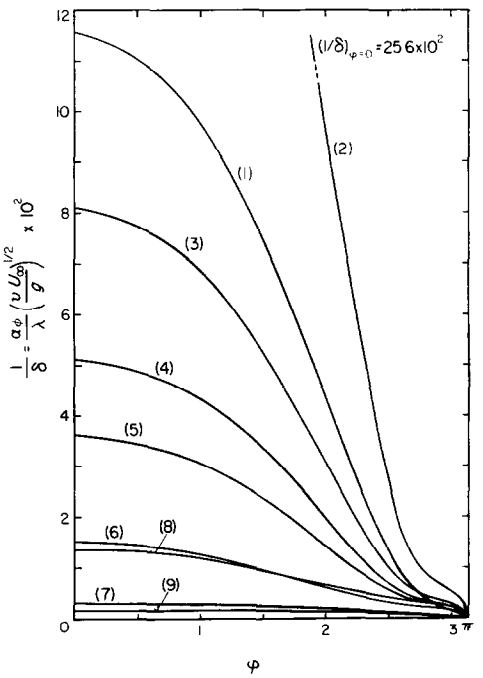

FIG. 2. Peripheral distributions of the nondimensional coefficients of heat transfer. Numbers in parentheses correspond to those in Table 1 respectively.

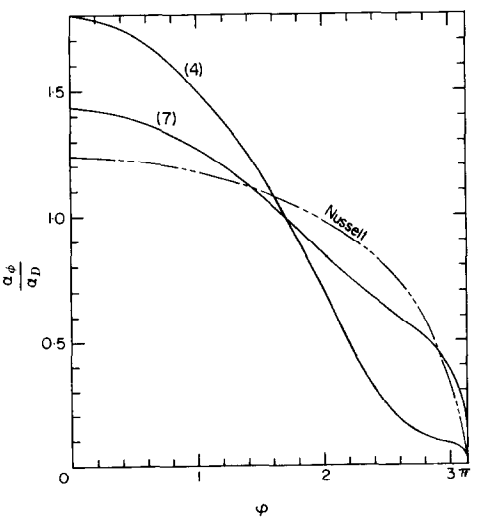

FIG. 3. Influence of oncoming vapour velocity upon distributions of local coefficients of heat transfer. Numbers in parentheses correspond to those in Table 1 respectively.

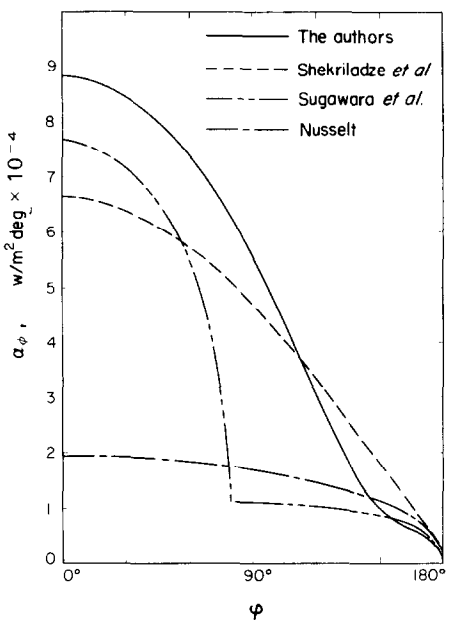

FIG. 4. Comparison among several solutions on local coefficients of heat transfer for a real condition of $U_\infty = 70$ m/s, $T_s - T_w = 2$ deg, $T_s = 30$°C and $D = 14$ mm.

In Fig. 4 the peripheral distributions of the local coefficients of heat transfer for a real condition given in the figure are compared among those calculated by means of the methods of the authors, Sugawara *et al.* [8], Shekriladze-Gomelauri [9] and Nusselt [1]. The solution by the authors gives the highest value in the average coefficient, and the least value in the local coefficient near the trailing stagnation. It seems that the latter fact is caused by thickening of the liquid film owing to smaller vapour velocity as well as increasing of total condensation rate. The fact that the curve of Sugawara *et al.* is folded at $\varphi = 80$ degrees indicates the effect of separation of the vapour boundary layer. On account of the tendency that the separation point must be more retarded in the boundary layer with suction, it is reasonable to consider that this solution will predict somewhat smaller value in average coefficient. The curve of Shekriladze-Gomelauri is calculated under the assumptions that the local shearing stress is equal to the momentum given up by the

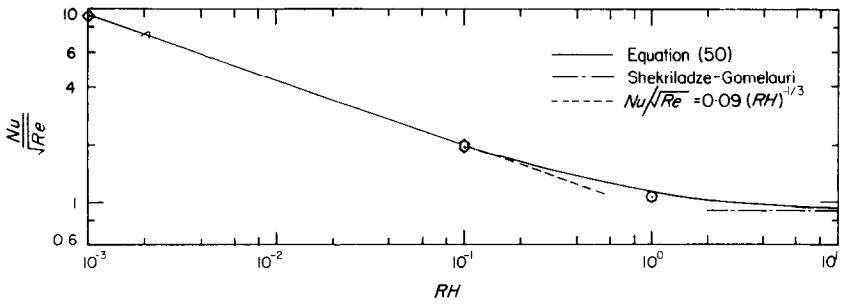

FIG. 5. Average Nusselt number in the case of large oncoming vapour velocity. Symbols correspond to those in Table 1 respectively.

condensing vapour and the effect of body force is negligibly small. From the results concerning a vertical plate it is considered that the average coefficients by this calculation has tendency to be underestimated generally.

The average coefficients of heat transfer for the case of relatively large oncoming vapour velocity are plotted in the relation of $Nu/\sqrt{Re}$ vs. RH in Fig. 5. These data may be expressed by

$$Nu = 0{\cdot}90\left(1+\frac{1}{RH}\right)^{\frac{1}{3}} Re^{\frac{1}{2}}, \quad RH < 10. \tag{50}$$

The data for the case of small oncoming vapour velocity tend to Nusselt's prediction, that is

$$Nu = 0{\cdot}725\left(\frac{Gr}{H}\right)^{\frac{1}{4}}, \tag{51}$$

where

$$Gr = \frac{D^3 g}{\nu^2}. \tag{52}$$

Such average Nusselt number Nu that becomes (50) and (51) in the limit cases of large and small oncoming vapour velocity respectively, is assumed as

$$Nu = \chi\left(1+\frac{0{\cdot}276}{\chi^4 FrH}\right)^{\frac{1}{4}} Re^{\frac{1}{2}}, \tag{53}$$

where

$$\chi = 0{\cdot}90\left(1+\frac{1}{RH}\right)^{\frac{1}{3}}. \tag{54}$$

In Fig. 6 numerical results are compared with (53). Maximum difference between these is about 5 per cent. The dotted line indicates

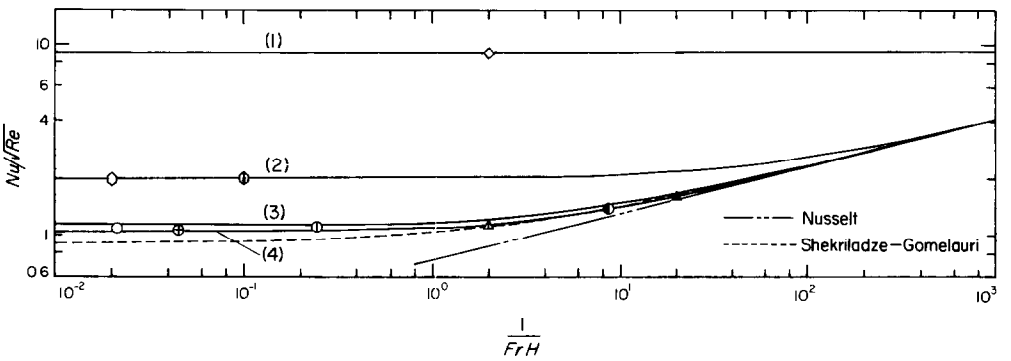

FIG. 6. Comparison between the numerical results and the values predicted by (53) on average Nusselt number. The curves (1), (2), (3) and (4) correspond to the cases of $RH = 10^{-3}$, 10^{-1}, 1 and 2 in (53) respectively. Symbols correspond to those in Table 1 respectively.

expression (28) in [9], which will be corresponding to the case of $RH \approx 10$ of calculation in this paper. Though (53) is generally available, (50) and (51) may be also adopted for the cases that U_∞ is much larger and much smaller than 0·276 $gD/\chi^4 H$ respectively.

Based on aforementioned results, the effect of pressure term neglected in (2) is considered. For an example of saturated steam at 20 deg C and a tube of 0·03 m dia., the ratio of pressure to body force term are expressed approximately as

$$4\bar{p}_\infty^2/\rho g D \approx 3 \times 10^{-4} U_\infty^2.$$

The ratios are about 0·03 and 1·2 for $U_\infty = 10$ m/s and 60 m/s respectively. For the case of relatively small oncoming vapour velocity, pressure term is negligibly small, and for large one, on the other hand, the magnitudes of both terms are comparable. For the latter case, however, the effect of pressure term also will become negligibly small, because the body force term is negligibly small in comparison with viscous one. Inclusively, the ignorance of pressure term in (2) is reasonable except narrow range near $U_\infty^2 \approx 0{\cdot}276\, gD/\chi^4 H$.

4. EXPERIMENTAL RESULTS

Experiments for condensation of steam were performed with a horizontal brass tube of 0·014 m o.d. and 0·0104 m i.d., which intersected through a circular duct of 0·092 m i.d. Eight thermocouples of 0·023 m effective length were inserted in the wall of the brass tube as shown in Fig. 7. Some experimental conditions and average Nusselt numbers measured are listed up in Table 2. The detail of the test loop is described in [12].

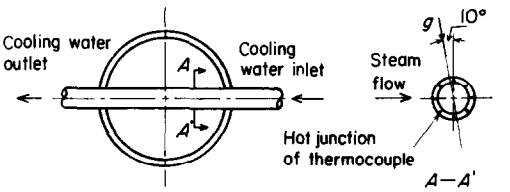

FIG. 7. Sketch of a heat transferring tube.

The temperature measured by i-th thermocouple T_i is nondimensionalized by $(T_i - T_m)/(T_s - T_m)$, and plotted as a function of angle φ in Fig. 8, where T_m is the arithmetic mean of T_i and T_s is the steam temperature. The peripheral distribution of wall temperature is

Table 2. Experimental results

Run	Symbol	T_{ci} (°C)	ΔT_c (deg)	w (m/s)	T_s (°C)	$T_s - T_w$ (deg)	U_∞ (m/s)	α_D (W/m² deg)	Nu_{exp}	Nu_{51}	Nu_{50}	Nu_{53}
1	○	10·12	0·61	1·04	22·07	1·01	71·3	$5{\cdot}35 \times 10^4$	1250	421	1270	1280
2	○	10·19	0·56	0·95	22·32	1·08	68·5	4·19	976	414	1240	1240
3	○	10·12	0·56	1·28	22·27	1·23	69·1	4·93	1150	400	1210	1210
4	○	10·91	0·49	1·02	22·22	1·04	55·8	4·06	945	418	1120	1120
5	⊢	5·28	0·54	0·82	20·31	1·00	36·3	3·79	889	418	889	899
6	⊢	5·75	0·59	0·82	20·75	1·05	35·4	4·00	931	414	873	884
7	◇	5·02	0·77	0·70	26·51	1·11	26·1	3·53	944	419	805	820
8	△	4·81	0·72	0·97	25·53	1·37	31·7	3·58	994	396	839	850
9	△	5·18	0·56	1·00	21·77	1·42	22·5	3·37	788	400	664	684
10	△	5·16	0·51	1·00	22·00	1·56	23·3	2·80	655	376	668	684
11	△	5·72	0·49	1·44	21·65	1·97	24·8	3·04	710	534	658	671
12	△	5·02	0·53	1·44	21·50	1·95	24·4	3·36	786	355	652	667
13	□	5·44	0·53	0·59	18·78	0·75	7·2			453	418	519

T_{ci}, temperature of cooling water at the inlet; ΔT_c, temperature rise of cooling water; w, velocity of cooling water; Nu_{51}, Nu_{50} and Nu_{53} are Nusselt numbers predicted by (51), (50) and (53) respectively.

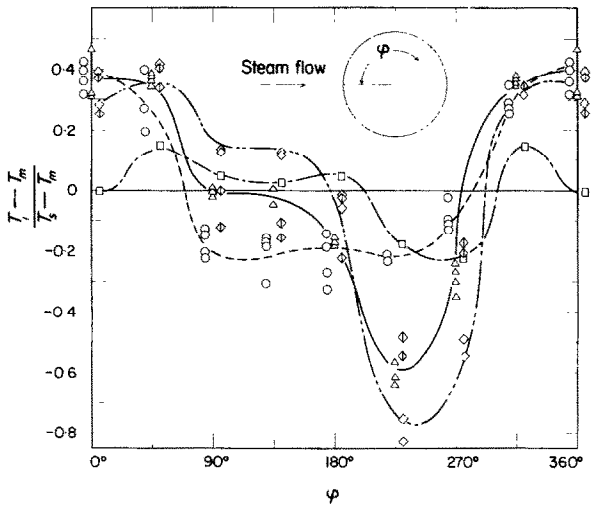

FIG. 8. Temperature distributions of tube wall. Symbols correspond to those in Table 2.

affected by both oncoming velocity U_∞ and heat flux q. Therefore, the relation between the temperature measured at a definite point and the peripheral mean value depends on experimental conditions. In Fig. 9 there are plotted the correlation between the arithmetic mean values of the readings at eight points $(T_s - T_m)_8$ and those of four points of every one skip $(T_s - T_m)_4$. The fact that the scattering of the correlation is within about three per cent suggests that the number of thermocouples inserted at peripheral equi-distance in the tube wall must be at least four in order to measure the peripheral mean temperature.

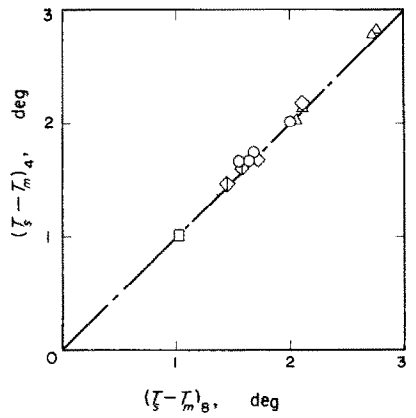

FIG. 9. Correlation between mean temperature differences of eight points $(T_s - T_m)_8$ and four points $(T_s - T_m)_4$. Symbols correspond to those in Table 2.

In Fig. 10 the average Nusselt number measured Nu_{exp} is compared with the values predicted by (51) for body force convection, (50) for forced convection and (53) for combined convection respectively. In these predictions there are used the measured values of the temperature and oncoming velocity of steam and the peripheral mean surface temperature of the tube wall corrected by the mean heat flux. Though the direction of steam flow is different from the situation of theoretical calculation and the experiments are not so accurate owing to small temperature rise in cooling water, the data are in fairly good agreement with (53) or (50). In each figure there are also plotted experimental data by Berman–Tumanov [13], which are the cases of downward and relatively low velocity of steam. These are in good agreement with (53) as shown in Fig. 10(c).

On the average coefficients of heat transfer, the fairly good agreement between the laminar theories treated in this paper and the experimental results suggests that the influence of turbulence in the liquid film or the vapour flow, if there were, is small.

5. CONCLUSIONS

(1) The average coefficients of heat transfer are expressed by (53). When oncoming vapour velocity is high, that is $U_\infty^2 \gg 0{\cdot}276\, gD/\chi^4 H$, the effect of parameter RH on the coefficients is remarkable but the effect of body force is negligible.

(2) As the oncoming vapour velocity becomes higher, the local coefficients of upper stream side become relatively higher. About 80 per cent of total condensation takes place in the upper half of the cylinder.

(3) In experiments, the temperature of tube wall is not uniform, but the peripheral distribution is affected by both oncoming vapour velocity and heat flux. In order to measure the

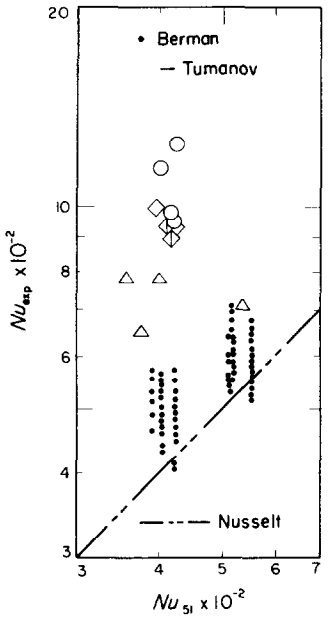

(a)

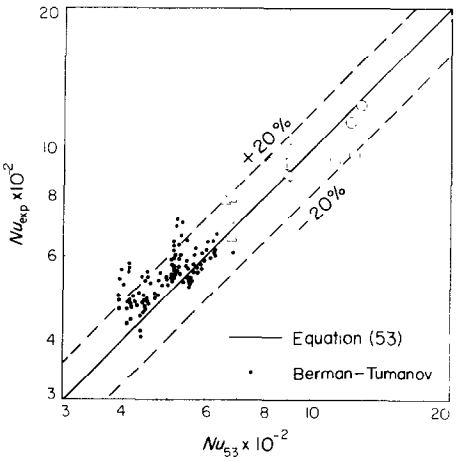

(c)

FIG. 10. Comparison between experimental average Nusselt numbers and theoretical ones. Symbols correspond to those in Table 2.
(a) experimental values vs. (51).
(b) experimental values vs. (50).
(c) experimental values vs. (53).

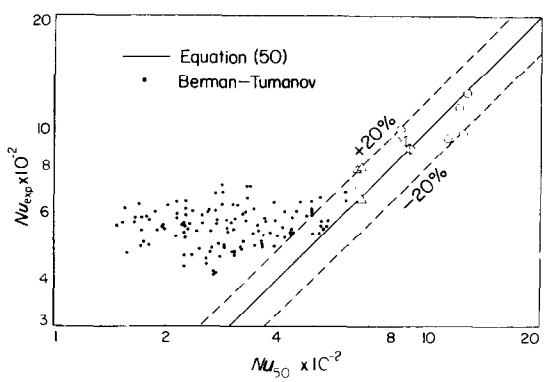

(b)

peripheral mean temperature, four thermocouples at least must be inserted at equi-distance in the tube wall. The mean value is employed for the prediction of the average coefficient of heat transfer.

(4) The agreement between theoretical and experimental results is fairly good on the average coefficients of heat transfer.

ACKNOWLEDGEMENTS

The authors acknowledge the help and participation of Mres. K. Hirata, K. Oda and M. Izumi in the manufacturing of the apparatus and the experiments. Numerical computations were performed with an electronic computer FACOM 230-60 in Computer Center, Kyūshū University.

REFERENCES

1. W. NUSSELT. Die Oberflächenkondensation des Wasserdampfes, *Z. ver. deut. Ing.* **60**, 541–580 (1916).
2. E. M. SPARROW and J. L. GREGG. Laminar condensation heat transfer on a horizontal cylinder, *Trans. Am. Soc. Mech. Engrs* **81C**, 291–296 (1959).
3. M. M. CHEN. An analytical study of laminar film condensation; Part 2—Single and multiple horizontal tubes, *Trans. Am. Soc. Mech. Engrs* **83C**, 55–60 (1961).
4. W. H. MCADAMS. *Heat Transmission*. 3rd Ed. p. 340. McGraw-Hill, New York, (1954).
5. J. ŠTĚPÁNEK, A. HEYBERGER und V. VESELÝ. Wärmeübergang am Wagrechten Rohr bei Kondensation gesättiger und Überhitzter Dämpfe. *Int. J. Heat Mass Transfer* **12**, 137–146 (1969).
6. B. E. SHORT and H. E. BROWN. Condensation of vapors on vertical banks of horizontal tubes. Proc. general discussion on heat transfer, pp. 27–31 (1957).

7. F. L. YOUNG and W. J. WOHLENBERG, Condensation of saturated Freon-12 vapor on a bank of horizontal tubes, *Trans. Am. Soc. Mech. Engrs* **64**, 787–794 (1942).
8. S. SUGAWARA, I. MICHIYOSHI and T. MINAMIYAMA, The condensation of vapor flowing normal to horizontal pipe, Proc. 6th Japan Nat. Congr. Appl. Mech. 1956, pp. 385–388 (1957).
9. I. G. SHEKRILADZE and V. I. GOMELAURI, Theoretical study of laminar film condensation of flowing vapor. *Int. J. Heat Mass Transfer* **9**. 581–591 (1966).
10. V. E. DENNY and A. F. MILLS, Laminar film condensation of a flowing vapor on a horizontal cylinder at normal gravity, *Trans. Am. Soc. Mech. Engrs* **91C**, 495–501 (1969).
11. T. FUJII and H. UEHARA, Laminar filmwise condensation on a vertical surface, *Int. J. Heat Mass Transfer* **15**, 217–233 (1972).
12. T. FUJII, H. UEHARA, K. HIRATA and K. ODA, Heat transfer and flow resistance in condensation of low pressure steam flowing through tube banks, *Int. J. Heat Mass Transfer*, **15**, 247–260 (1972).
13. L. D. BERMAN and U. A. TUMANOV, Issledovanie teplootdachi pri kondensatsii dvijushtshegosa para na gorizontalinoi trube, *Teploenergetika* **10**, 77–83 (1962).

CONDENSATION EN FILM LAMINAIRE D'UNE VAPEUR CIRCULANT AUTOUR D'UN CYLINDRE HORIZONTAL

Résumé—On a résolu les équations de la couche limite biphasique pour une condensation en film sur un cylindre horizontal en utilisant une méthode approchée due à Jacobs. Les résultats numériques relatifs aux coefficients moyens de transfert de chaleur sont exprimés comme suit:

pour un écoulement de vapeur vers le bas,

$$Nu = \chi\left(1 + \frac{0{,}276}{\chi^4 FrH}\right)^{\frac{1}{4}} Re^{\frac{1}{4}}$$

spécialement pour une grande vitesse de la vapeur et plus précisément pour

$$\frac{gD}{U_\infty^2 H} \ll \frac{\chi^4}{0{,}276}$$

$$Nu = \chi\, Re^{\frac{1}{4}}$$

$$\text{où } \chi = 0{,}9\left(1 + \frac{1}{RH}\right)^{\frac{1}{4}}.$$

Les coefficients de transfert thermique estimés par ces expressions sont en bon accord avec les résultats expérimentaux des auteurs et de Berman–Tumanov. La distribution de température sur le cylindre est généralement affectée par la vitesse de la vapeur et le flux thermique pariétal: par suite la température moyenne périphérique peut être considérée comme étant représentative.

LAMINARE FILMKONDENSATION VON STRÖMENDEM DAMPF AN EINEM WAAGERECHTEN ROHR

Zusammenfassung—Zwei-Phasen-Grenzschichtgleichungen für die Filmkondensation an einem horizontalen Rohr werden mit Hilfe einer Näherungsmethode nach Jacob gelöst.

Die numerischen Ergebnisse für mittlere Wärmeübergangs-Koeffizienten lassen sich wie folgt ausdrücken: für Dampfströmung nach unten:

$$Nu = \chi\left(1 + \frac{0{,}276}{\chi^4 FrH}\right)^{\frac{1}{4}} Re^{\frac{1}{4}}$$

Besonders für grösse Dampfgeschwindigkeiten, nämlich wenn

$$\frac{g \cdot D}{w_\infty^2 H} \ll \frac{\chi^4}{0{,}276} \text{ ist, kann geschrieben werden:}$$

$$Nu = \chi \cdot Re^{\frac{1}{4}} \text{ mit } \chi = 0{,}9\left(1 + \frac{1}{RH}\right)^{\frac{1}{4}}.$$

Die hiermit errechneten Wärmeübergangskoeffizienten stimmen gut mit den experimentellen Werten überein, die von den Autoren diesen Arbeit und von Berman-Tumanov gemessen wurden.

Die Temperaturverteilung am Zylinder wird gewöhnlich von der herrschenden Dampfgeschwindigkeit und vom Wärmestrom durch die Oberfläche beeinflusst. In diesem Fall muss die mittlere Temperatur des Umfangs als Bezugstemperatur herangezogen werden.

ЛАМНИАРНАЯ ПЛЕНОЧНАЯ КОНДЕНСАЦИЯ ПАРА, ДВИЖУЩЕГОСЯ ПО ГОРИЗОНТАЛЬНОМУ ЦИЛИНДРУ

Аннотация—С помощью приближенного метода Джекобса решаются уравнения двухфазного пограничного слоя для пленочной конденсации на горизонтальном цилиндре. Численные результаты для средних значений коэффициента переноса тепла выражаются следующим образом:
для направленного вниз потока пара

$$Nu = \chi \left(1 + \frac{0{,}276}{\chi^4 Fr\bar{H}}\right)^{1/4} Re^{1/2}$$

в особенности для большой скорости пара, а именно для $gD/W_\infty{}^2 H \ll \chi^4/0{,}276$

$$Nu = \chi\, Re^{1/2}$$

где $\chi = 0{,}9(I + 1/RH)^{1/3}$

Коэффициенты переноса тепла, рассчитанные с помощью этих выражений, хорошо согласуются с экспериментальными данными, полученными авторами и Берманом-Тумановым. Распределение температуры по цилиндру находится под влиянием скорости набегающего потока пара и тепла к поверхности. Тогда за характерные значения должны приниматься средние значения температуры по периферии.